



Cite this: *Mater. Adv.*, 2024,  
5, 9417

## Development and characterisation of starch/alginate active films incorporated with lemongrass essential oil (*Cymbopogon citratus*)†

Olga Lucía Torres Vargas,<sup>✉</sup> \* Yessica Viviana Galeano Loaiza<sup>✉</sup> and  
Iván Andrés Rodríguez Agredo<sup>✉</sup>

The development of active films based on biopolymers containing antimicrobial and antioxidant compounds has contributed to the improvement of food safety. In the present study, the composition of lemongrass (*Cymbopogon citratus*) essential oil (LEO) was evaluated by gas chromatography-mass spectrometry (GC-MS) analysis and the minimum inhibitory concentration (MIC) against *S. aureus* and *E. coli* bacteria was determined. Films based on cassava starch and sodium alginate were prepared incorporating different concentrations (0.0, 0.5, 1.0, and 1.5%) of lemongrass essential oil (FLEO). Their physicochemical, mechanical, optical, retention and release properties, as well as their antibacterial and antioxidant activities were evaluated. GC/MS analysis of lemongrass essential oil (LEO) revealed the presence of citral (39.12%) and citronellol (34.47%) as major components. A minimum inhibitory concentration (MIC) of 25  $\mu\text{g mL}^{-1}$  was observed for LEO against *S. aureus* and *E. coli* bacteria. A significant decrease (12.42%) in water vapour permeability (WVP), moisture content (12.68%) and solubility (18.47%) was found as the LEO concentration in the films increased. Scanning electron microscopy (SEM) analyses showed a uniform distribution of LEO in the films, while FTIR spectra revealed interactions between the components. X-ray diffraction (XRD) patterns indicated that the incorporation of LEO did not affect the structural stability of the films, showing a decrease in crystallinity of 8.4%. Furthermore, The results showed an antioxidant activity of 32.4%, bacteriostatic activity against *S. aureus* and *E. coli* and a more stable release and retention of essential oil (EO) in films containing 1.5% LEO. These results suggest that the developed films have potential for application in active packaging.

Received 11th June 2024,  
Accepted 27th October 2024

DOI: 10.1039/d4ma00608a

rsc.li/materials-advances

## 1. Introduction

The growing need for food packaging systems that can retard or inhibit microbial growth, extend food shelf life and align with sustainable development goal 12 (ONU),<sup>1</sup> manifests itself in the search for solutions that reduce the ecological footprint. This approach involves the transition from conventional plastic production methods to the efficient use of biopolymers in the production of active and biodegradable films, thus contributing to more sustainable and environmentally friendly practices.<sup>2</sup>

In this context, the development of biodegradable active films is of increasing interest due to their composition based on natural biopolymers such as polysaccharides, including

starch, alginate, pectin and gums, the combination of which often gives the films flexibility.<sup>3</sup> In addition, these active films have shown good barrier properties, biocompatibility, renewability and biodegradability.<sup>4</sup> In turn, these films can incorporate biologically active compounds, such as essential oils, which can inhibit microbial growth and reduce oxygen penetration, with the underlying purpose of prolonging shelf life and improving food quality.<sup>5</sup>

Essential oils are secondary metabolites found in the leaves, bark, stems, roots, flowers, or fruits of plants.<sup>6</sup> A variety of essential oils are currently of great interest in the food industry due to their antioxidant and antimicrobial properties.<sup>7</sup> Among them, lemongrass essential oil (LEO) has been highlighted for its functional properties.<sup>8</sup> Among them, lemongrass essential oil (LEO) has been highlighted for its functional properties.<sup>8</sup> This oil is a type of essential oil with a strong lemon flavour extracted from the plant *Cymbopogon citratus*, commonly known as lemongrass, which is widely distributed in the tropics and subtropics.<sup>9</sup> The main compound in LEO is citral, which has antimicrobial, antifungal and antioxidant properties.<sup>10</sup>

Group of Research on Agro-industrial Sciences, Interdisciplinary Science Institute, Food Engineering Laboratory, Universidad del Quindío. Cra. 15# 12 N, Armenia, Quindío, 630004, Colombia. E-mail: oltorres@uniquindio.edu.co

† Electronic supplementary information (ESI) available. See DOI: <https://doi.org/10.1039/d4ma00608a>



On the other hand, cassava starch is one of the most abundant and biodegradable polysaccharides and is widely used in film development. Its combination with other biopolymers has been shown to improve physical, mechanical and barrier properties. Among these biopolymers is sodium alginate, a naturally occurring anionic polysaccharide found in the intercellular matrix of brown algae that is generally recognised as safe (GRAS). This biopolymer has properties that include the ability to form uniform gels and/or thicken the solution and provide barrier properties.<sup>3</sup>

Therefore, the objective of this study was to evaluate the effect caused by the inclusion of lemongrass essential oil in a film made from cassava starch and sodium alginate on its physicochemical, mechanical, optical, retention and release properties, as well as its antibacterial and antioxidant activity.

## 2. Materials and methods

### 2.1 Raw material

Lemongrass (*Cymbopogon citratus*) essential oil (LEO) was purchased from Tecnas S.A., Colombia. The cassava starch was obtained using the methodology described by J. Aristizábal *et al.*<sup>11</sup> Sodium alginate (PanReac AppliChem, Darmstadt, Germany). Calcium chloride ( $\text{CaCl}_2$ ), glycerol, tween 80 and the different reagents necessary for the physical and microbiological characterization of the formulated films were acquired from Merck in Colombia.

### 2.2 Gas chromatography-mass spectrometry (GC-MS) analysis

The chemical composition of lemongrass essential oil (LEO) was determined by gas chromatography-mass spectrometry (GC-MS). An Agilent HP-6890N gas chromatograph coupled to an Agilent 5973N mass selective detector (Agilent Technologies, HP USA), equipped with a DB-1 M capillary column (30 m long  $\times$  0.25 mm internal diameter and  $\times$  0.25  $\mu\text{m}$  film thickness) was used. Helium (99.999%) was used as the carrier gas at a flow rate of 1.0  $\text{mL min}^{-1}$  and an injector temperature of 250 °C. 0.2  $\mu\text{L}$  of the lemongrass oil was injected in split mode. The oven temperature programme was at 70 °C for 10 min, increased to 100 °C at 5 °C  $\text{min}^{-1}$ , followed by an increase to 150 °C at 5 °C  $\text{min}^{-1}$ , then to 200 °C at 5 °C  $\text{min}^{-1}$  and finally to 250 °C at 5 °C  $\text{min}^{-1}$  for 15 min.

Mass spectra were recorded in electron impact ionisation mode at 70 eV. The temperatures of the quadrupole mass detector, ion source and transfer line were set at 150, 230 and 280 °C respectively. Compound identification was based on the mass spectra (MS) obtained with those from the NIST02.L, NIST5a.L and NIST98.L libraries and the selected ion monitoring mode was used to determine the concentrations of the compounds.

### 2.3 Bacterial strains and growth conditions

The bacterial strains *Staphylococcus aureus* (ATCC 25923) and *Escherichia coli* (ATCC 25922) were obtained from the culture collection of the Molecular Immunology Research Group (GYMOL) of the Universidad del Quindío. *S. aureus* and *E. coli*

cultures were preserved in 18% glycerol and kept at  $-80\text{ }^{\circ}\text{C}$  until use. The inocula were separately grown in 10 mL of nutrient broth for 18 hours at 35 °C under aerobic conditions. Subsequently, the cultures were adjusted to a density of 0.5 on the McFarland scale ( $\cong 1 \times 10^8\text{ CFU mL}^{-1}$ ) before being used on *in vitro* antibacterial tests.

### 2.4 Minimum inhibitory concentrations (MIC)

Minimum inhibitory concentration (MIC) assays were performed using the broth microdilution method in Mueller-Hilton (MH) medium, according to M. Fadli *et al.*<sup>12</sup> Lemongrass essential oil (LEO) was analysed using a series of double dilutions prepared in 1% dimethyl sulfoxide (DMSO) at concentrations ranging from 3.125 to 100  $\mu\text{g mL}^{-1}$ . From the initial densities, an adjustment was made to obtain an approximate final inoculum size of  $5 \times 10^5\text{ CFU mL}^{-1}$ , for the bacteria by adding to each well a volume of 0.1 mL. On the other hand, the microtiter plates were sealed with a sterile adhesive film to avoid any loss of essential oil due to its inherent volatility.

The microtiter plates were incubated under optimal conditions (37 °C for 24 h).<sup>13</sup> After incubation, 30  $\mu\text{L}$  of 0.02% resazurin was added to each well and further incubated for 24 h to observe the colour change. Viable microorganisms that interact with the indicator by changing from blue to pink denote bacterial growth. Therefore, the lowest dilution without a blue colour change is considered the MIC for LEO.<sup>14</sup> All results were calculated as the means of experiments performed in triplicate.

### 2.5 Film formulation

The materials and the methodology that were used in this research to obtain the films were based on previous studies.<sup>15,16</sup> Initially, 3.6 g of cassava starch were added to 72 g of distilled water at 70 °C with constant agitation at 600 rpm for 30 min. In parallel, 2.4 g of sodium alginate were dissolved in 72 g of distilled water at 60 °C for 30 min. Then a  $\text{CaCl}_2$  solution was added dropwise (0.01%  $\text{CaCl}_2$  was added for each gramme of sodium alginate). Both solutions were mixed with constant agitation for 15 min. Subsequently, the 15% glycerol solution (w/w, with respect to the weight of cassava starch) was brought to  $35 \pm 5\text{ }^{\circ}\text{C}$  for 15 min.

Tween 80 at 5% (w/w, based on LEO) was used as a surfactant and once the solution mixtures were obtained, LEO was added at concentrations of 0.5, 1.0, and 1.5% (w/w total solids). These concentrations were selected base on the minimum inhibitory concentration (MIC) determined in this study and those reported in the literature.<sup>17,18</sup>

The mixture was homogenised in Ultraturrax (IKA T25, Staufen, Germany) at 12 000 rpm for 5 min at room temperature. It was then subjected to ultrasonic cleaner Branson-1510 (Danbury, CT, USA) for 30 min at 40 kHz frequency.

The obtained film-forming solution (SFP) was distributed on polystyrene Petri dishes (18 g) (64  $\text{cm}^2$ ) and dried in a forced air convection oven (Binder, FD-115, Germany) at  $45 \pm 5\text{ }^{\circ}\text{C}$  for 6 h. A control film (CF) was prepared following the same methodology, without adding LEO. All films (CF: Control Film,



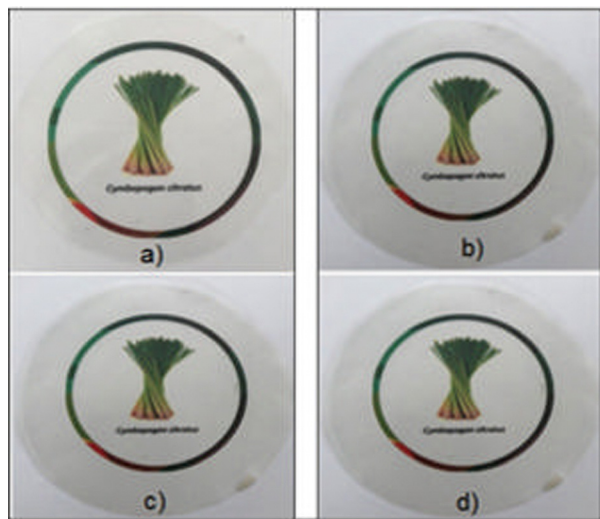


Fig. 1 Visual appearance of the films (a) CF, (b) FLEO-0.5%, (c) FLEO-1.0%, (d) FLEO-1.5%.

FLEO: Film with lemongrass essential oil) were stored in a desiccator at  $23 \pm 2$  °C and  $50 \pm 2\%$  relative humidity (RH) for subsequent analyses Fig. 1 shows the images of the films obtained.

## 2.6 Characterization of the films

**2.6.1 Thickness and mechanical properties.** The thickness of the FLEOs was measured using a digital micrometre with an accuracy of 0.001 mm (Mitutoyo, Corp, Ltdy col., Tokyo, Japan). Five measurements were taken at randomly selected points on each type of film obtained; the value of each thickness was the average of the measurements taken.

The mechanical properties of the films were measured in a texturometer (TA, XT2, Textura Technologies Corp col., Scarsdale, NY, USA). Tensile strength (TS) and elongation at break (EB, %) were determined until rupture of the FLEOs. The samples were die cut into  $2\text{ cm} \times 6\text{ cm}$  sheets and conditioned for 48 h at  $25 \pm 0.2$  °C and  $50 \pm 1\%$  relative humidity. During the analysis, they were subjected to tension with a 40 mm separation between the grips. Tensile strength and elongation were calculated according to ASTM D882-01 (ref. 19) of the American Society for Testing and Materials.

**2.6.2 Water vapour permeability, moisture content and solubility.** To determine water vapour permeability (WVP), the FLEOs were conditioned for 48 h at  $20 \pm 0.1$  °C and a relative humidity of  $40 \pm 1\%$ . It was evaluated according to ASTM E-96 (ref. 20) of the American Society for Testing and Materials. The capsules were weighed every hour for 9 h in order to determine the weight loss of the films.

Moisture content was determined by the gravimetric method,<sup>21</sup> conditioning for 48 h at 25 °C at 50% relative humidity. The samples were cut into  $2\text{ cm} \times 2\text{ cm}$  films and weighed. Initially, the weight of the films was taken ( $W_m$ ) subsequently, they were placed in a drying oven (Binder, FD-115, Germany) at 105 °C for 24 h to constant weight ( $W_d$ ).

The moisture content was calculated using eqn (1).

$$\text{Moisture content} = \frac{W_m - W_d}{W_d} \times 100 \quad (1)$$

The solubility of FLEOs was determined by the percentage of the film dry matter that is soluble in water. The methodology reported by R. Akhter *et al.*<sup>22</sup> was followed with some modifications. FLEOs were cut into  $2\text{ cm} \times 2\text{ cm}$  sheets. The samples were dried at 105 °C to a constant weight to obtain the initial dry mass ( $M_1$ ). The FLEOs were placed in 50 mL of distilled water, covered and stored at 25 °C for 24 h, then vacuum filtered and dried at 105 °C to a constant weight to obtain the final dry mass ( $M_2$ ). Solubility was calculated using eqn (2).

$$\text{Solubility (\%)} = \frac{M_1 - M_2}{M_1} \times 100 \quad (2)$$

**2.6.3 Colour and opacity.** The colour evaluation of the FLEOs was performed with a Minolta CM-2002R photocolourimeter (Minolta Camera Coy col., Osaka, Japan), using a D65 illuminant and a 10° standard observer.<sup>23</sup> Colour determination and expression were performed based on CIEL\*a\*b\* coordinates and reflectance values.<sup>24</sup> Luminosity ( $L^*$ ), red-green ( $a^*$ ), and yellow-blue ( $b^*$ ) parameters were obtained directly from the equipment.

The opacity of the films was determined by the ratio of films superimposed on a white ( $L^*$ white) and black ( $L^*$ black) plate, according to eqn (3).<sup>25</sup>

$$\text{Opacity} = \frac{L^*_{\text{black}}}{L^*_{\text{white}}} \times 100 \quad (3)$$

**2.6.4 X-ray diffraction (XRD).** The XRD patterns of the obtained films were analysed on a D8 Advance X-ray diffractometer (Bruker AXS, Germany) with Co K $\alpha$  radiation of 1.544 nm wavelength at 40 kV and 15 mA. The film samples were scanned in the diffraction angle range ( $2\theta$ ) from 5 to 60° with a step size of 0.02°. The relative crystallinity was calculated by dividing the crystalline area by the total area.

**2.6.5 Fourier transformed infrared spectroscopy.** The interactions between the components of the films were performed by Fourier transform infrared spectroscopy (FTIR). The optical characterization of the films was performed by Fourier transform infrared spectroscopy (FTIR). The spectra of the samples were obtained in wavenumber ranges from 4000 to 400  $\text{cm}^{-1}$  using a PerKinElmer Spectrum (Mod. Spectrum Two, Waltham, MA, USA) equipped with a single-reflection diamond crystal ATR module. Spectra were recorded in a spectral range between 400 and 4000  $\text{cm}^{-1}$  at a scan rate of 32 scans and a spectral resolution of 4  $\text{cm}^{-1}$ .

**2.6.6 Scanning electron microscopy (SEM).** The morphology of CF and FLEO-0.5%, FLEO-1.0% and FLEO-1.5% was analysed using scanning electron microscopy (JEOL model JSM-6610LV, Japan). Samples of  $4\text{ mm} \times 4\text{ mm}$  were used to obtain images of the surface and cross section of the films. Images were captured using an accelerating voltage of 5 kV and



observed at 1000 $\times$  magnification. All samples were coated with gold prior to observation.

## 2.7 Retention and release study

**2.7.1 Retention of LEO in the film.** LEO retention during film storage (25  $^{\circ}$ C, 50% RH) was quantified using the method of T. Xu *et al.*,<sup>26</sup> with some modifications. Initially, 0.5g of the film was placed in a centrifuge tube containing ultrapure water (5 mL) and anhydrous ethanol (15 mL). It was then left in agitation overnight at 25  $^{\circ}$ C. The solution was then centrifuged at 6000 rpm for 30 min to extract the supernatant. The absorbance of the supernatant was measured at a wavelength of 325 nm using a UV-vis spectrophotometer (Agilent HP-8453). LEO concentration was calibrated using a standard curve of LEO in ethanol. Measurements were taken once a day for 15 days. LEO loss was calculated according to eqn (4).

$$\text{Loss (\%)} = \frac{C - C_t}{C} \times 100 \quad (4)$$

where  $C$  is the initial amount of LEO and  $C_t$  is the amount of LEO after storage of films for  $t$  days.

**2.7.2 FLEO release profile.** The release rate of LEO-incorporated films was quantified using the method of T. Xu *et al.*<sup>26</sup> with some modifications. A 60% (v/v) glycerol solution was used as an aqueous food simulant (water activity approximately 0.6 to 0.7). Films (0.5 g) were cut into equal parts and immersed in 30 mL of the simulant solution with constant agitation at 50 rpm at 25  $^{\circ}$ C. Subsequently, at intervals of 5, 10, and 30 min for 2 h, 1 mL of solution was extracted and dissolved in ethanol to measure the absorbance at a wavelength of 240 nm by UV-vis spectrophotometer (Agilent HP-8453).

## 2.8 Antioxidant activity

Several techniques have been employed to evaluate the antioxidant capacity of functional foods, such as herbal extracts and natural or synthetic compounds. These techniques include the diphenylpicrylhydrazyl (DPPH) free radical assay, the ferric reducing activity power (FRAP) assay, and the 2,2'-azinobis-(3-ethylbenzothiazoline-6-sulfonic acid) (ABTS) assay. Among these, the DPPH antioxidant assay is widely used due to the high stability, experimental feasibility, and low cost of the DPPH radical.<sup>27,28</sup>

The antioxidant activity of the obtained films was evaluated by 2,2-diphenyl-1-picryl-hydrazyl (DPPH) free radical scavenging assay according to the methodology of M. Moradi *et al.*<sup>29</sup> with some modifications.

First, 25 mg of film was immersed in 3 mL of deionised water. The resulting mixture was stirred at room temperature for 15 h, followed by centrifugation at 4185  $\times g$  for 15 min. The resulting film extracts (2.8 mL) were mixed with 0.1 mL of 1 M methanol solution of DPPH, and left in the dark at 25  $^{\circ}$ C for 30 min. The absorbance of the mixture was measured in a spectrophotometer at 515 nm; the absorbance of the solution without film (blank) was also measured. The percentage inhibition or reduction of the DPPH radical from the radical

scavenging activity of DPPH was calculated using eqn (5).

$$AA = \frac{\text{Abs DPPH} - \text{Abs film extract}}{\text{Abs DPPH}} \times 100 \quad (5)$$

where: AA (%) is the percentage inhibition or reduction of the DPPH radical, Abs DPPH is the absorbance value at 515 nm of the methanolic solution of DPPH and film extract, Abs is the absorbance value at 515 nm for each formulated film.

## 2.9 Antibacterial activity

The antimicrobial activity of the films obtained was determined using the agar disc diffusion method described by S. K. Bajpai *et al.*<sup>30</sup> with some modifications. The growth conditions of the bacterial strains were performed according to numeral 2.3.

Discs of 5 mm diameter of the films (previously sterilised on each side for 5 min with UV-C light: 254 nm) were placed on Mueller-Hinton solid agar previously spread on the surface with 100  $\mu$ L of 10<sup>8</sup> CFU mL<sup>-1</sup> of the suspensions with the bacterial cultures of *S. aureus* (ATCC 25923) and *E. coli* (ATCC 25922). The Petri dishes were incubated at 37  $^{\circ}$ C for 24 h. The diameter of the inhibition zones of the discs (mm) was measured using a digital calliper (Mitutoyo no. 192-30, Tokyo, Japan).

## 2.10 Statistical analysis

Statistical analysis of the data was performed by analysis of variance (ANOVA) using Statgraphics Centurion XVIII. One-way ANOVA and Tukey's multiple comparison tests were used to classify and assess statistical differences in ranges. In all cases,  $p < 0.05$  was considered significant. All the experiments were performed in triplicate.

# 3. Results and discussion

## 3.1 Gas chromatography-mass spectrometry (GC-MS) analysis

The chemical composition of LEO is shown in Table 1. A total of 41 compounds were identified in LEO by GC-MS analysis, representing 99.82% of the total volatile compounds. The most abundant compound was citral (39.12%), followed by citronellol (34.47%), citronellal (4.74%), caryophyllene (2.83%) and limonene (2.79%).

These results differ from the main compounds reported by G. Antonioli *et al.*,<sup>31</sup> which were geranial (41.8%), neral (25.6%) and  $\beta$ -myrcene (18.1%). Similarly, neral (34.48%), geranial (34.37%) and  $\beta$ -myrcene (12.84%) were reported as the major components of lemongrass oil.<sup>32</sup> Another study reported citral (70.22%) and myrcene (13.64%) as the major constituents of LEO.<sup>33</sup> Therefore, the variation in the components of oils obtained from plant matrices is due to various factors (differences in harvesting season, geography, plant populations, edaphic factors, and extraction methods).<sup>34</sup>

## 3.2 Minimum inhibitory concentration (MIC)

The MIC values obtained for LEO against *S. aureus* (Gram-positive) and *E. coli* (Gram-negative) bacteria are shown in Fig. 2. For both bacteria, LEO exhibited a MIC starting at 25  $\mu$ g mL<sup>-1</sup>. Similarly, one study reported a MIC of 3125  $\mu$ g mL<sup>-1</sup> for both *S. aureus*





Table 1 Compounds identified of lemongrass essential oil (LEO)

Compound	Retention time (min)	Relative content (%)
5-Hepten-2-one, 6-methyl-	5.29	0.94
$\alpha$ -Sabinene	5.42	0.10
$\beta$ -Myrcene	5.62	0.25
1S- $\alpha$ -Pinene	6.10	0.22
Limonene	6.50	2.79
(E)- $\beta$ -Ocimene	6.57	0.49
(Z)- $\beta$ -Ocimene	6.81	0.26
Phenol, <i>m</i> -tert-butyl-	8.34	0.08
Linalool	8.06	0.67
Cis-rose oxide	8.34	0.09
Cyclohexene, 3,3,5-trimethyl-	8.99	0.13
1,4-Hexadiene, 3,3,5-trimethyl-	9.29	0.38
(R)-(+)-Citronellal	9.68	4.74
3-Decyne	9.98	1.40
Imidazole, 5-[N(2)-(isopropylidene)carbhydrazino]-	10.33	0.06
Cyclohexanone, 5-methyl-2-(1-methylethenyl)-, <i>trans</i>	10.63	1.86
1,11-Dodecadiene	10.91	0.02
Decanal	11.50	0.26
(R)-(+)- $\beta$ -Citronellol	13.40	34.47
Citral	14.71	39.12
<i>cis</i> -2,6-dimethyl-2,6-octadiene	16.82	0.71
Geranyl acetate	17.71	2.30
Trans-nerolidol	18.03	0.08
(-)- $\beta$ -Elemene	18.26	0.38
Caryophyllene	19.15	2.83
4,7,10-Cycloundecatriene, 1,1,4,8-tetramethyl-, <i>cis</i> , <i>cis</i> , <i>cis</i> -	19.99	0.36
Germacrene D	20.76	0.44
$\alpha$ -Muurolene	21.33	0.14
$\gamma$ -Muurolene	21.74	0.21
$\delta$ -Cadinene	22.06	0.70
$\alpha$ -Elemol	22.84	0.64
1-Hydroxy-1,7-dimethyl-4-isopropyl-2,7-cyclodecadiene	23.95	0.71
Caryophyllene oxide	24.06	0.62
3-Octyne, 7-methyl-	25.02	0.10
$\gamma$ -Eudesmol	26.19	0.07
$\tau$ -Muurolol	26.61	0.43
$\beta$ -Eusdemol	26.90	0.05
$\alpha$ -Cadinol	27.16	0.55
7-Octen-1-ol, 2,6-dimethyl-	34.04	0.07
1,5,9-Decatriene, 2,3,5,8-Tetramethyl-	37.83	0.04
Neoisolongifolene, 8-bromo-	41.47	0.06
Total		99.82

and *E. coli*.<sup>35</sup> In contrast, MIC values of 63  $\mu\text{g mL}^{-1}$  were found for *E. coli* and 125  $\mu\text{g mL}^{-1}$  for *S. aureus*.<sup>13</sup> Another study has reported an MIC of 2200  $\mu\text{g mL}^{-1}$  to inhibit the planktonic growth of *E. coli*.<sup>36</sup> Viktorová *et al.*<sup>37</sup> reported MIC values of 5190  $\mu\text{g mL}^{-1}$  for the Gram-positive bacterium *S. aureus*, and 2125  $\mu\text{g mL}^{-1}$  and 2338  $\mu\text{g mL}^{-1}$  for the Gram-negative bacteria *Pseudomonas aeruginosa* and *Salmonella enterica*, respectively.

The antibacterial activity of LEO is attributed to its ability to alter cell membrane integrity, inducing changes in membrane permeability and the release of cell contents, leading to cell death.<sup>38</sup> Additionally, the antibacterial activity of LEO has been attributed to citral (a blend of neral and geranial) as the main antibacterial agent against Gram-positive and Gram-negative bacteria.<sup>37</sup> However, other components of LEO may influence its biological properties by altering or modifying the effects of other compounds, potentially contributing to synergistic activity.<sup>39–41</sup> Furthermore, although the antimicrobial efficacy of LEO is mainly determined by the concentration of bacteria and the oil content, other factors can also influence its effectiveness. These factors include the composition of the oil, the

method of extraction, the stage of development of the plant and the environmental conditions.<sup>42</sup>

### 3.3 Characterization of the films

**3.3.1 Thickness and mechanical properties.** The results obtained for the thickness, tensile strength (TS) and elongation at break (EB) of the films are presented in Table 2. The thickness values obtained ranged from  $0.090 \pm 0.02$  to  $0.107 \pm 0.03$  mm without significant changes ( $p > 0.05$ ). Similar results have been observed in pectin films with copaiba oil.<sup>43</sup> Similarly, no change was observed in the thickness of an edible gelatine-chitosan coating with LEO.<sup>44</sup>

The addition of LEO to the films presented significant differences ( $p < 0.05$ ) in mechanical properties compared to CF (Table 2). Tensile strength (TS) and elongation at break (EB) decreased with increasing LEO concentration. This effect can be attributed to the reduction in component interactions, leading to differences in the cross-linking of the polymer matrix.<sup>45</sup> These results are consistent with the slight changes observed in XRD and SEM analyses.



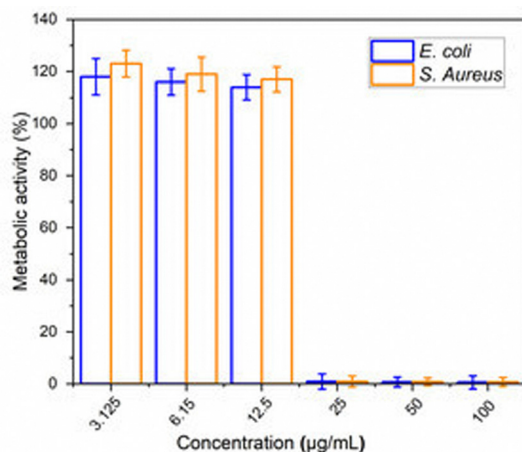


Fig. 2 Minimum inhibitory concentration (MIC) of lemongrass essential oil (LEO) at different concentrations ( $3.125\text{--}100\ \mu\text{g mL}^{-1}$ ) against *S. aureus* and *E. coli*. Data shown represent mean  $\pm$  standard deviation. Different letters on the bars indicate significant differences between groups ( $p < 0.05$ ) based on one-way ANOVA followed by Tukey test.

Table 2 Thickness and mechanical properties of the films containing or not different concentrations of lemongrass oil essential (LEO)<sup>ab</sup>

Film	Thickness (mm)	TS (MPa)	EB (%)
CF	$0.107 \pm 0.03^*$	$2.15 \pm 0.57^*$	$14.08 \pm 1.57^*$
FLEO 0.5%	$0.095 \pm 0.01^*$	$1.49 \pm 0.43^{**}$	$11.85 \pm 1.18^{**}$
FLEO 1.0%	$0.090 \pm 0.02^*$	$1.35 \pm 0.09^{***}$	$10.78 \pm 1.26^{**}$
FLEO 1.5%	$0.107 \pm 0.03^*$	$1.31 \pm 0.60^{****}$	$10.57 \pm 1.05^{**}$

<sup>a</sup> Data reported are mean values  $\pm$  standard deviation. <sup>b</sup> Median on the same column with a different number of asterisks are significantly different (Tukey:  $p < 0.05$ ).

A decrease in TS and EB has been reported in chitosan films with natural extracts.<sup>46</sup> Similarly, higher TS and EB were observed in the control film (cassava starch/chitosan) compared to films incorporated with LEO.<sup>14</sup> F. Han Lyn and Z. A. Nur Hanani<sup>47</sup> also found a decrease in TS with increasing LEO concentration in chitosan films. On the contrary, EB increased with increasing LEO concentration in the films.

**3.3.2 Water vapour permeability, moisture content and solubility.** The values of water vapour permeability (WVP) and moisture content shown in Table 3 ranged between  $6.84 \pm 0.30 \times 10^{-9}\ \text{g s}^{-1}\ \text{m}^{-1}\ \text{Pa}^{-1}$  and  $7.81 \pm 0.52 \times 10^{-9}\ \text{g s}^{-1}\ \text{m}^{-1}\ \text{Pa}^{-1}$  and  $17.76 \pm 0.20\%$  and  $20.34 \pm 0.50\%$ , respectively. WVP and moisture content were higher for CF compared to FLEOs. A slight decrease ( $p < 0.05$ ) was observed with increasing LEO concentration. This suggests that the inclusion of LEO may reduce the diffusion of water molecules through the polymeric matrix, due to the reduction of free spaces in the film by the formation of intermolecular forces between the essential oil and the other components. This helps to reduce the moisture content and consequently improves the barrier properties of the film.<sup>48,49</sup> A decrease in WVP was also observed in cassava starch-based films with LEO compared to the control film.<sup>17</sup>

Regarding the solubility of the films (Table 3), a decrease ( $p < 0.05$ ) was evidenced with increasing LEO concentration.

Table 3 Water vapour permeability (WVP), moisture content and solubility of the films containing or not different concentrations of lemongrass oil essential (LEO)<sup>ab</sup>

Film	WVP ( $\times 10^{-9}\ \text{g s}^{-1}\ \text{m}^{-1}\ \text{Pa}^{-1}$ )	Moisture content (%)	Solubility (%)
CF	$7.81 \pm 0.52^*$	$20.34 \pm 0.50^*$	$85.05 \pm 0.91^*$
FLEO 0.5%	$6.92 \pm 0.38^{**}$	$18.41 \pm 0.33^{**}$	$78.72 \pm 0.78^{**}$
FLEO 1.0%	$6.87 \pm 0.25^{**}$	$17.95 \pm 0.40^{***}$	$73.30 \pm 1.32^{***}$
FLEO 1.5%	$6.84 \pm 0.30^{**}$	$17.76 \pm 0.20^{***}$	$69.34 \pm 1.23^{****}$

<sup>a</sup> Data reported are mean values  $\pm$  standard deviation. <sup>b</sup> Median on the same column with a different number of asterisks are significantly different (Tukey:  $p < 0.05$ ).

The highest solubility was found in CF ( $85.05 \pm 0.91\%$ ) compared to FLEO-0.5% ( $78.72 \pm 0.78\%$ ), FLEO-1.0% ( $73.30 \pm 1.32\%$ ) and FLEO-1.5% ( $69.34 \pm 1.23\%$ ). This is attributed to the fact that LEO reduces the amount of OH bonds, leading to the formation of hydrophobic regions in the polymer matrix, which results in lower solubility by hindering water penetration through the material.<sup>22</sup> In addition, active films have been shown to have barrier properties against water vapour and oxygen.<sup>50</sup>

Similar results were obtained by F. Han Lyn and Z. A. Nur Hanani,<sup>47</sup> who reported a decrease in WVP, moisture content and solubility with increasing LEO concentration in chitosan films. Similarly, a decrease in moisture content, solubility, and WVP was reported for films made from potato starch, Zedo gum, and *Salvia officinalis* essential oil.<sup>51</sup> Also, A. Istiqomah *et al.*<sup>18</sup> observed a decrease in moisture content and solubility by adding LEO to chitosan and *Dioscorea hispida* starch-based films.

**3.3.3 Colour and opacity.** The values of the colour parameters ( $L^*$ ,  $a^*$  and  $b^*$ ) and the opacity of the films are shown in Table 4. Luminosity ( $L^*$ ) decreased slightly with increasing LEO concentration, with values between  $56.77 \pm 0.06$  and  $55.20 \pm 0.17$ , whereas the value of parameter  $b^*$  (blue/yellow) increased slightly with increasing LEO concentration, with values between  $16.37 \pm 0.12$  and  $17.17 \pm 0.23$ .

As for the values of  $a^*$  (green/red) and opacity, no significant differences were observed. However, the films showed opacity values between  $78.12 \pm 0.16$  and  $79.59 \pm 0.93$ . These values suggest a potential application for light-sensitive foods, as opacity is a desirable property that provides a barrier to visible light, thus helping to prevent light-induced lipid oxidation.<sup>52</sup>

In general, the incorporation of LEO did not affect the colour parameters ( $L^*$ ,  $a^*$  and  $b^*$ ) and opacity of the films ( $p > 0.05$ ). These results are probably due to the light colour of LEO and the low concentrations of essential oil. Similar results have been reported for corn starch films with orange and *Zanthoxylum bungeanum* essential oils.<sup>53,54</sup> In contrast, one study reported an increase in  $L^*$ ,  $a^*$  and  $b^*$  colour parameters when lemon essential oil was incorporated into films based on grass carp collagen and chitosan.<sup>55</sup>

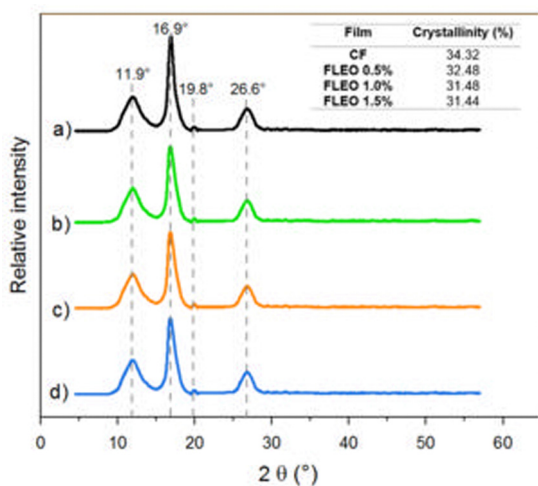
**3.3.4 X-ray diffraction (XRD).** X-ray diffractograms of the films are shown in Fig. 3. CF and FLEO showed a faint peak at  $2\theta = 19.8^\circ$ , two broad peaks at  $11.9$  and  $26.6^\circ$  and a high



**Table 4** CIELAB colour parameters and opacity of the films containing or not different concentrations of lemongrass oil essential (LEO)<sup>ab</sup>

Film	<i>L</i> *	<i>a</i> *	<i>b</i> *	Opacity (%)
CF	56.77 ± 0.06*	1.10 ± 0.10*	16.37 ± 0.12*	78.37 ± 0.60*
FLEO	55.63 ± 0.11**	1.09 ± 0.08*	16.53 ± 0.10**	78.12 ± 0.16*
0.5%				
FLEO	55.57 ± 0.15**	1.10 ± 0.00*	16.60 ± 0.16**	79.01 ± 1.00**
1.0%				
FLEO	55.20 ± 0.17***	1.10 ± 0.06*	17.17 ± 0.23***	79.59 ± 0.93**
1.5%				

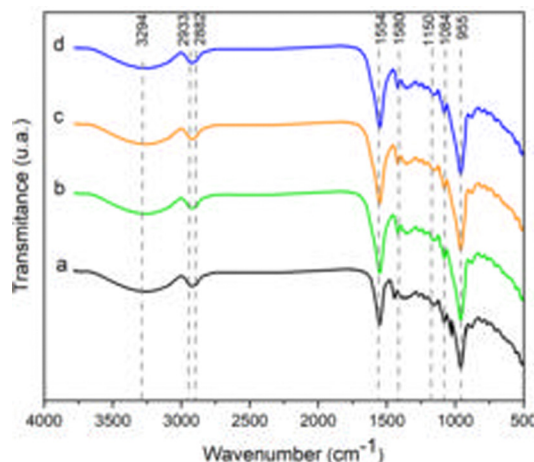
<sup>a</sup> Data reported are mean values ± standard deviation. <sup>b</sup> Median on the same column with a different number of asterisks are significantly different (Tukey: *p* < 0.05).

**Fig. 3** XRD patterns of the films (a) CF (b) FLEO-0.5%, (c) FLEO-1.0% and (d) FLEO-1.5%.

intensity peak at  $2\theta = 16.9^\circ$ . However, the inclusion of LEO resulted in a slight decrease in crystallinity of 5.36% (FLEO-0.5%), 8.28 (FLEO-1.0%) and 8.4% (FLEO-1.5%) with respect to CF, suggesting a change in the interplanar spacing, associated with the inclusion of LEO.<sup>43</sup>

In general, the incorporation of LEO did not cause significant changes in the microstructure of the films. Consistent with these results, a study showed that the addition of 1% cinnamon oil to pinto bean starch and polyvinyl alcohol films did not affect the position of the peaks compared to the control film.<sup>56</sup> Similarly, in corn starch films with LEO, the presence of LEO was found not to affect the crystallographic structure of the films.<sup>57</sup> In contrast, the incorporation of thyme oil into a soy protein isolate based film resulted in a less crystalline structure.<sup>58</sup>

**3.3.5 Fourier transformed infrared spectroscopy (FTIR).** The FTIR spectra of the functional groups and intermolecular interactions of the film components are shown in Fig. 4. The bands between 3683 and 3063  $\text{cm}^{-1}$  related to the O–H stretching of water molecules and hydroxyl groups of the film components<sup>59</sup> showed slight changes in intensity and length with increasing LEO in the films. This suggests the formation

**Fig. 4** FTIR spectra of the films (a) CF, (b) FLEO-0.5%, (c) FLEO-1.0% and (d) FLEO-1.5%.

of new intermolecular hydrogen bonds between LEO, starch and sodium alginate.<sup>18</sup>

The bands at 2933 and 2882  $\text{cm}^{-1}$  are attributed to antisymmetric and symmetric stretching vibrations of the  $-\text{CH}_3$  and  $-\text{CH}_2$  bonds. In addition, spectral changes in these bands are associated with lipids, surfactants and an increase in ester group content upon incorporation of essential oil.<sup>60,61</sup>

The bands at 1554 and 1380  $\text{cm}^{-1}$  are attributed to bending and stretching vibrations of the O–H groups of matrix-bound water.<sup>62</sup> However, a higher intensity at 1554  $\text{cm}^{-1}$  has been observed in FLEOs, associated with compounds present in LEO.<sup>17,63</sup>

The bands identified at 1150, 1084 and 1027  $\text{cm}^{-1}$  correspond to stretching frequencies of C–O groups associated with C–O–C glycosidic bonds.<sup>64</sup> The band located at 955  $\text{cm}^{-1}$  corresponds to the stretching vibration of the pyranose ring.<sup>65</sup> The observed changes in the position of the bands between 1150 and 955  $\text{cm}^{-1}$  suggest an interaction of hydrogen bonds between starch, alginate, glycerol and LEO.<sup>66</sup> Bands below 868  $\text{cm}^{-1}$  are attributed to skeletal vibrations of the glucopyranose rings.<sup>67</sup>

**3.3.6 Scanning electron microscopy (SEM).** SEM images of the surface and cross section of CF and FLEO-1.5% are shown in Fig. 5. The films showed a smooth, homogeneous, uniform surface with no pore formation or cracks. In cross-section, CF showed a more compact structure compared to FLEO-1.5%, which had a rough appearance and uniform LEO distribution.

These results are consistent with the findings obtained from mechanical, optical, and barrier properties, as well as FTIR and XRD analysis. The interaction between the film components affects the microstructure of the polymer matrix, which directly impacts the mechanical, optical, physical and barrier properties.<sup>68</sup> Previous research on cassava starch-based films and chitosan and sodium alginate coatings with cinnamon essential oil observed a microstructure with uniform distribution of the essential oil.<sup>61,69</sup> Similarly, Bansal *et al.*<sup>70</sup> observed smooth and homogeneous structures in an edible coating of buckwheat starch with xanthan gum and LEO.



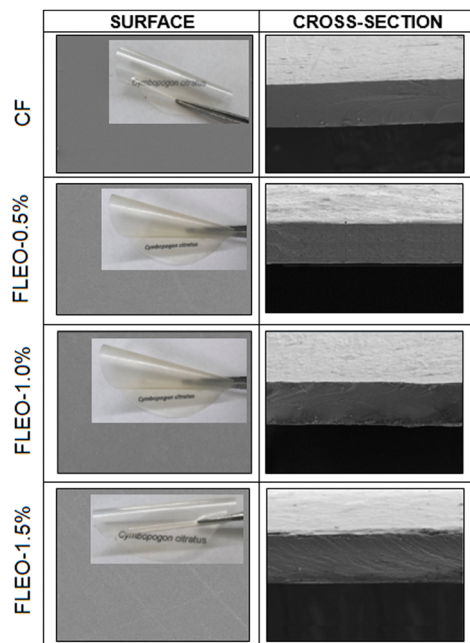


Fig. 5 SEM images of the surface (left column) and the cross-sections (right column) of the film CF, FLEO-0.5%, FLEO-1.0% and FLEO-1.5%.

### 3.4 Retention and release study

**3.4.1 Retention of LEO in the films.** Fig. 6 shows the loss of LEO retention of the films during storage time. During the first 6 days, oil release of up to 65%, 53% and 26% was observed for FLEO-0.5%, FLEO-1.0% and FLEO-1.5% films respectively. After 6 days of storage, a trend towards sustained or continuous LEO release (slower release) was evident, with an amount of oil released from the FLEO-0.5%, FLEO-1.0%, and FLEO-1.5% films of approximately 74, 68, and 61%, respectively, at 15 days.

The results showed significant differences ( $p < 0.05$ ) of the films during the storage time, demonstrating that FLEO-1.5%

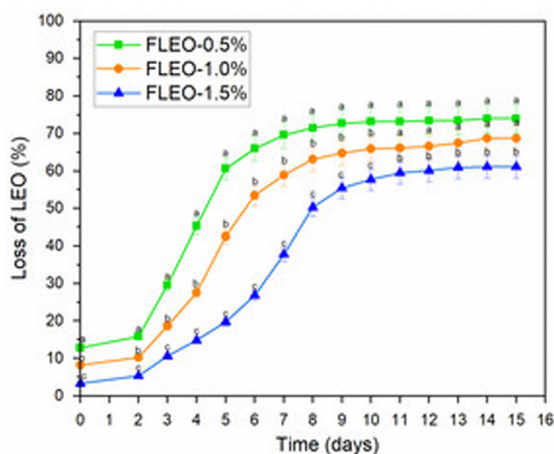


Fig. 6 Loss of lemongrass essential oil (LEO) from the films: FLEO-0.5%, FLEO-1.0% and FLEO-1.5%. Different letters on the bars indicate significant differences between treatments ( $p < 0.05$ ) based on one-way ANOVA followed by Tukey test.

showed a higher retention of LEO in the polymeric matrix compared to FLEO-1.0% and FLEO-0.5%, which could be attributed to an increase in chemical interactions between LEO and the other components of the polymeric matrix.<sup>71</sup>

In addition, the compatibility between the components of the film and their uniform distribution (SEM Fig. 5) leads to a significant stability and retention of the essential oil. P. B Kavur and A. Yemencioğlu<sup>72</sup> showed that chitosan films with chick-pea proteins, which had a more homogeneous distribution of eugenol droplets in the films, had a higher retention. On the contrary, Zhu *et al.*<sup>73</sup> observed an increase in thymol release in bilayer films with increasing oil addition during storage time.

**3.4.2 FLEO release profile.** The *in vitro* release profile of LEO is shown in Fig. 7. All films showed a similar release trend, however, FLEO-05% showed a slightly higher release rate (79%) compared to FLEO-1.0% and FLEO-1.5%, which showed a 2 h release rate of 73 and 71%, respectively.

An initial rapid release of LEO was also observed when the films were immersed in the simulant solution, which could be attributed to the easy and rapid penetration of the simulant solution into the polymer matrix. Subsequently, the release rate decreased during the remaining period. This behaviour was also observed in polyvinyl alcohol/gum arabic gum/chitosan composite films with black pepper essential oil and ginger essential oil incorporated.<sup>71</sup>

Therefore, the diffusion of essential oils through the film matrix is also influenced by the swelling process, which creates a more open structure and consequently increases the mobility and release of the essential oil. Similarly, the interaction between the components of the polymeric matrix with the active substances and the characteristics of the simulant are factors that promote the release of this type of substance.<sup>46,74</sup>

### 3.5 Antioxidant activity

The DPPH radical inhibition activity of films with and without LEO addition is shown in Fig. 8. CF showed no antioxidant

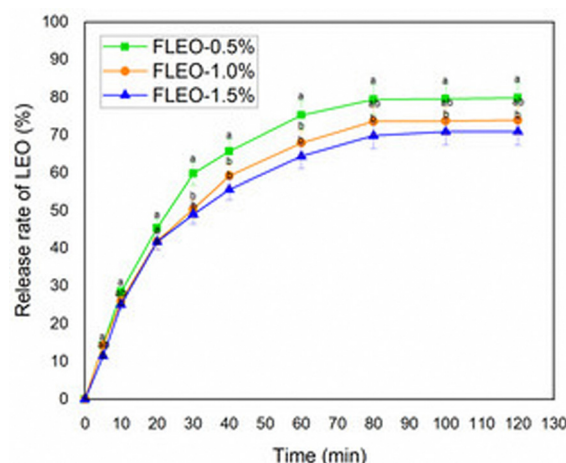


Fig. 7 Release profile of lemongrass essential oil (LEO) from the films: FLEO-0.5%, FLEO-1.0% and FLEO-1.5%. Different letters on the bars indicate significant differences between treatments ( $p < 0.05$ ) based on one-way ANOVA followed by Tukey test.





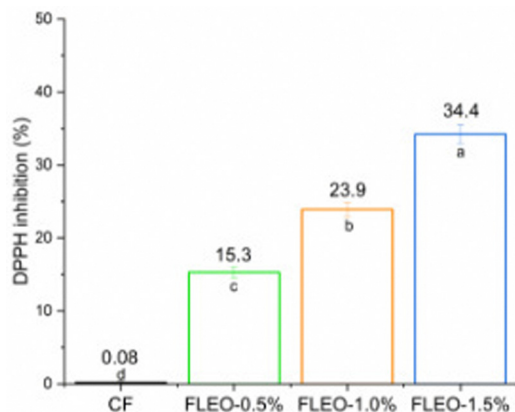


Fig. 8 DPPH inhibition activity of the films containing or not different concentrations of lemongrass essential oil (LEO). Different letters on the bars indicate significant differences between treatments ( $p < 0.05$ ) based on one-way ANOVA followed by Tukey test.

activity, whereas LEO incorporation resulted in a significant increase ( $p < 0.05$ ) with increasing LEO concentration. This is mainly attributed to citral, as it has been shown to be effective in scavenging free radicals and has the ability to donate hydrogen atoms to allylic sites.<sup>75</sup> In addition, the presence of secondary metabolites and phenolic acids in LEO has been reported to confer antioxidant capacity.<sup>57</sup> However, the antioxidant capacity of LEO, as well as its antimicrobial activity, may vary due to several factors, such as the extraction method, the origin of the species and the part of the plant used for extraction.<sup>76</sup>

A study on polyvinyl alcohol and cassava starch-based films reported an increase in antioxidant capacity with increasing LEO concentration.<sup>9</sup> Similarly, an increase in antioxidant activity was shown for the sweet potato starch film incorporated with LEO.<sup>77</sup> An increasing trend in radical scavenging was also observed with higher oil concentrations.<sup>78</sup>

### 3.6 Antibacterial activity

Increasing the concentration of LEO in the film shows a significant increase ( $p < 0.05$ ) in antibacterial activity (Table 5). In contrast, CF showed no zone of inhibition. The results show that FLEOs have antibacterial properties against *S. aureus* (Gram-positive) and *E. coli* (Gram-negative). This antibacterial effect is

Table 5 Antibacterial activity of the films containing or not different concentrations of lemongrass essential oil (LEO) against *S. aureus* and *E. coli*.<sup>a,b</sup>

Film	Inhibition zone (mm)	
	<i>S. aureus</i>	<i>E. coli</i>
CF	0.0*	0.0*
FLEO 0.5%	15.92 ± 1.03**	13.96 ± 0.98**
FLEO 1.0%	17.13 ± 1.09***	14.10 ± 1.12**
FLEO 1.5%	19.24 ± 1.18****	16.06 ± 1.27***

<sup>a</sup> Data reported are mean values ± standard deviation. <sup>b</sup> Median on the same column with a different number of asterisks are significantly different (Tukey:  $p < 0.05$ ).

attributed to the fact that LEO induces damage to the cell membrane of bacteria, interfering with their growth and reproduction, ultimately leading to cell death.<sup>42,79,80</sup>

In addition, slightly higher inhibition zones (between  $15.92 \pm 1.03$  and  $19.24 \pm 1.18$ ) were observed for *S. aureus* compared to *E. coli* (between  $13.96 \pm 0.98$  and  $16.06 \pm 1.27$ ). This is attributed to the fact that the composition of the cell wall of Gram-negative bacteria can reduce the effect of essential oils. This is because they have a thin layer of peptidoglycan and an outer membrane composed of lipoproteins, which acts as a barrier against hydrophilic compounds.<sup>81</sup> A similar behaviour was observed in films of chitosan, *Dioscorea hispida* starch and LEO, which showed a higher antibacterial activity against Gram-positive bacteria (*S. aureus* and *S. epidermis*) compared to Gram-negative bacteria (*E. coli* and *S. typhi*).<sup>18</sup> Another study also showed an increase in inhibition zones against *S. aureus* and *E. coli* with increasing LEO concentration in an edible coating of buckwheat starch with xanthan gum.<sup>70</sup> In addition, Socaciu *et al.*<sup>82</sup> observed a higher zone of inhibition for *S. aureus* in whey protein and Tarragon essential oil based films compared to *E. coli*.

## 4. Conclusions

In this study, citral and citronellol, were identified as the major components of lemongrass essential oil (LEO) with a minimum inhibitory concentration (MIC) of  $25 \mu\text{g mL}^{-1}$  against *S. aureus* and *E. coli* bacteria. Incorporation of LEO into the films resulted in a decrease in water vapour permeability (WVP), moisture content and solubility with increasing LEO concentration.

No effect on mechanical properties and colour parameters was observed when LEO was incorporated into the films. SEM, FTIR and XRD analyses confirmed the intermolecular interactions between LEO, starch, sodium alginate and glycerol. The results of *in vitro* release studies, antioxidant and antibacterial activities in FLEO-1.5% indicate the viability of the active films for food applications.

Therefore, the study of materials with natural composites for food packaging has great potential for implementation in the food industry, driving the development of active films to extend the shelf life of food and reduce the use of synthetic materials, in line with the trends towards sustainability and food safety.

## Author contributions

Olga Lucía Torres Vargas – funding acquisition, conceptualization, writing – reviewing and editing; Yessica Viviana Galeano Loaiza – formal analysis, data curation, conceptualization, validation and writing; Iván Andrés Rodríguez Agredo – supervision, methodology and investigation.

## Data availability

The data supporting this article have been included as part of the ESI.†



## Conflicts of interest

There are no conflicts to declare.

## Acknowledgements

We thank the Molecular Immunology Research Group (GYMOL) of the Universidad del Quindío for their collaboration in the analysis of the Minimum Inhibitory Concentration (MIC) and for providing the bacterial strains necessary for this study. We would like to thank the Vicerrectoria de Investigaciones at Universidad del Quindío for providing financial support (Research Project No. 1073).

## References

- 1 ONU. *Objetivo 12: Garantizar modalidades de consumo y producción sostenibles*, <https://www.un.org/sustainabledevelopment/es/sustainable-consumption-production/>, 2020.
- 2 B. Haridevamuthu, D. Raj, A. Chandran, R. Murugan, S. Seetharaman, M. Dhanaraj and J. Arockiaraj, *Carbohydr. Polym.*, 2024, **329**, 121798.
- 3 Z. Hernández-Nolasco, M. A. Ríos-Corripio, J. V. Hidalgo-Contreras, P. H. Castellano, E. Rubio-Rosas and A. S. Hernández-Cázares, *LWT-Food Sci. Technol.*, 2024, **192**, 115718.
- 4 A. G. Sethulakshmi and M. P. Saravanakumar, *Int. J. Biol. Macromol.*, 2024, **260**, 129153.
- 5 Z. Song, J. Wei, Y. Cao, Q. Yu and L. Han, *Food Chem.*, 2023, **418**, 135958.
- 6 M. A. Hanif, S. Nisar, G. S. Khan, Z. Mushtaq and M. Zubair, *J. Essent. Oil Res.*, 2019, 3–17.
- 7 Z. Liu, S. Wang, H. Liang, J. Zhou, M. Zong, Y. Cao and W. Lou, *Int. J. Biol. Macromol.*, 2024, 133242.
- 8 J. Jovanović, J. Čirković, A. Radojković, N. Tasić, D. Mutavdžić, G. Branković and Z. Branković, *Int. J. Biol. Macromol.*, 2024, 133335.
- 9 Z. Chen, L. Zong, C. Chen and J. Xie, *Food Packag. Shelf Life*, 2020, **26**, 100565.
- 10 A. D. Sharma, I. Kaur and A. Chauhan, *Chem. Afr.*, 2023, **6**, 2835–2848.
- 11 J. Aristizábal, T. Sánchez and D. M. Lorío. *Guía técnica para producción y análisis de almidón de yuca*, 2007, 49–59, <https://www.fao.org/3/a1028s/a1028s00.htm>.
- 12 M. Fadli, J. M. Bolla, N. E. Mezrioui, J. M. Pagès and L. Hassani, *Ind. Crops Prod.*, 2014, **61**, 370–376.
- 13 A. Ahmad and A. Viljoen, *Phytomedicine*, 2015, **22**(6), 657–665.
- 14 M. I. Perdana, J. Ruamcharoen, S. Panphon and M. Leelakriangsak, *LWT-Food Sci. Technol.*, 2021, **141**, 110934.
- 15 O. L. Vargas, Y. V. Loaiza and M. Gonzalez, *J. Mater. Res. Technol.*, 2021, **13**, 2239–2250.
- 16 O. L. Vargas, I. A. Agredo and Y. V. Loaiza, *RSC Adv.*, 2024, **14**(22), 15293–15301.
- 17 J. F. Mendes, L. B. Norcino, H. H. A. Martins, A. Manrich, C. G. Otoni, E. E. N. Carvalho, R. H. Piccoli, J. E. Oliveira, A. C. M. Pinheiro and L. H. C. Mattoso, *Food Hydrocolloids*, 2020, **100**, 105428.
- 18 A. Istiqomah, W. E. Prasetyo, M. Firdaus and T. Kusumaningsih, *Int. J. Biol. Macromol.*, 2022, **210**, 669–681.
- 19 ASTM, *Standard test method for tensile properties of thin plastic sheeting*, in *Standard Designations D882-01, Annual Book of ASTM Standards*, American Society for Testing and Materials, Philadelphia, PA, 2002.
- 20 ASTM, *Standard test methods for water vapor transmission of materials*, in *E96 e 05, Annual Book of ASTM Standards*, American Society for Testing and Materials, 2005.
- 21 AOAC Association of Official Agricultural Chemists, *Official Methods of Analysis of AOAC International*, AOAC International Rockville, USA, 20th edn, 2016.
- 22 R. Akhter, F. A. Masoodi, T. A. Wani and S. A. Rather, *Int. J. Biol. Macromol.*, 2019, **137**, 1245–1255.
- 23 UNE 40-080, *Determinación de las magnitudes cromáticas CIE*, Norma española, Instituto Español de Normalización (IRANOR), Madrid, 1984.
- 24 CIE, *Industrial colour-difference evaluation*, Technical report 116/1995, Commission Internationale de l'Eclairage Central Bureau, Vienna, Austria, 1995.
- 25 Hunter Associates Laboratory, *Universal software versions 3.2 and above: User's manual: manual version 1.5*, Reston, 1997.
- 26 T. Xu, C. Gao, Y. Yang, X. Shen, M. Huang, S. Liu and X. Tang, *Food Hydrocolloids*, 2018, **84**, 84–92.
- 27 C. Han, P. Jin, M. Li, L. Wang and Y. Zheng, *J. Agric. Food Chem.*, 2017, **65**, 7159–7167.
- 28 M. Parcheta, R. Świsłocka, S. Orzechowska, M. Akimowicz, R. Choińska and W. Lewandowski, *Mater.*, 2021, **14**(8), 1984.
- 29 M. Moradi, H. Tajik, S. M. Rohani and A. Mahmoudian, *LWT-Food Sci. Technol.*, 2016, **72**, 37–43.
- 30 S. K. Bajpai, N. Chand and V. Chaurasia, *Food Bioprocess Technol.*, 2012, **5**, 1871–1881.
- 31 G. Antonioli, G. Fontanella, S. Echeverrigaray, A. P. L. Delamare, G. F. Pauletti and T. Barcellos, *Food Chem.*, 2020, **326**, 126997.
- 32 M. D. T. Ngongang, P. Eke, M. L. Sameza, M. N. L. N. Mback, C. D. Lordon and F. F. Boyom, *Int. J. Trop. Insect Sci.*, 2022, 1–13.
- 33 S. A. Alsakhawy, H. H. Baghdadi, M. A. El-Shenawy and L. S. El-Hosseiny, *Sci. Rep.*, 2024, **14**(1), 17278.
- 34 A. Yadav, T. S. Raghuvanshi and B. Prakash, *Sustainable Food Technol.*, 2023, **1**(6), 930–940.
- 35 D. Babatunde, G. Otusemade, M. Ojewumi, O. Agboola, E. Oyeniyi and K. Akinlabu, *Inter. J. Mech. Eng. Technol.*, 2019, **10**(3), 882–889.
- 36 L. A. Ortega-Ramirez, M. M. Gutiérrez-Pacheco, I. Vargas-Arispuro, G. A. González-Aguilar, M. A. Martínez-Téllez and J. F. Ayala-Zavala, *Antibiotics*, 2020, **9**(3), 102.
- 37 J. Viktorová, M. Stupák, K. Řehořová, S. Dobiasová, L. Hoang, J. Hajšlová, T. Thanh, L. Tri, N. Tuan and T. Ruml, *Foods*, 2020, **9**(5), 585.
- 38 V. Valková, H. Ďuranová, L. Galovičová, P. Borotová, N. L. Vukovic, M. Vukic and M. Kačániová, *Agronomy*, 2022, **12**(1), 155.
- 39 R. Ribeiro-Santos, M. Andrade, N. R. de Melo and A. Sanches-Silva, Use of essential oils in active food



- packaging: Recent advances and future trends, *Trends Food Sci. Technol.*, 2017, **61**, 132–140.
- 40 J. Sharifi-Rad, A. Sureda, G. C. Tenore, M. Daglia, M. Sharifi-Rad, M. Valussi, R. Tundis, M. Sharifi-Rad, M. Loizzo, A. O. Ademiluyi, R. Sharifi-Rad, S. A. Ayatollahi and M. Iriti, *Molecules*, 2017, **22**(1), 70.
  - 41 Y. Zhang, J. Wei, H. Chen, Z. Song, H. Guo, Y. Yuan and T. Yue, *LWT–Food Sci. Technol.*, 2020, **117**, 108667.
  - 42 M. Mukarram, S. Choudhary, M. A. Khan, P. Poltronieri, M. M. A. Khan, J. Ali, D. Kurjak and M. Shahid, *Antioxidants*, 2021, **11**(1), 20.
  - 43 L. B. Norcinao, J. F. Mendes, C. V. L. Natarelli, A. Manrich, J. E. Oliveira and L. H. Mattoso, *Food Hydrocolloids*, 2020, **106**, 105862.
  - 44 T. Erceg, O. Šovljanski, A. Stupar, J. Ugarković, M. Aćimović, L. Pezo, A. Tomić and M. A. Todosijević, *Inter. J. Biol. Macromol.*, 2023, **228**, 400–410.
  - 45 M. Eltabakh, H. Kassab, W. Badawy, M. Abdin and S. Abdelhady, *J. Polym. Environ.*, 2021, **30**, 1–11.
  - 46 T. T. Nguyen, B. T. T. Pham, H. N. Le, L. G. Bach and C. H. Thuc, *Food Packag. Shelf Life*, 2022, **32**, 100830.
  - 47 F. Han Lyn and Z. A. Nur Hanani, *J. Package Technol. Res.*, 2020, **4**, 33–44.
  - 48 H. Almasi, S. Azizi and S. Amjadi, *Food Hydrocolloids*, 2020, **99**, 105338.
  - 49 B. Wang, J. Sui, B. Yu, C. Yuan, L. Guo, A. M. Abd El-Aty and B. Cui, *Carbohydr. Polym.*, 2021, **254**, 117314.
  - 50 Y. Liu, S. Kang, H. Zhang, Y. Kai and H. Yang, *Int. J. Food Microbiol.*, 2023, **407**, 110437.
  - 51 M. Pirouzifard, R. A. Yorghlanlu and S. Pirs, *J. Thermoplast. Compos. Mater.*, 2020, **33**(7), 915–937.
  - 52 X. Sun, H. Zhang, J. Wang, M. Dong, P. Jia, T. Bu, Q. Wang and L. Wang, *Food Packag. Shelf Life*, 2021, **29**, 100741.
  - 53 J. A. do Evangelho, G. da Silva Dannenberg, B. Biduski, S. L. M. El Halal, D. H. Kringel, M. A. Gualarte, A. M. Fiorentini and E. da Rosa Zavareze, *Carbohydr. Polym.*, 2019, **222**, 114981.
  - 54 Q. Yang, F. Zheng, Q. Chai, Z. Li, H. Zhao, J. Zhang, K. Nishinari and B. Cui, *Int. J. Biol. Macromol.*, 2024, **256**, 128382.
  - 55 Y. Jiang, W. Lan, D. E. Sameen, S. Ahmed, W. Qin, Q. Zhang, H. Chen, H. Dai, J. He and Y. Liu, *Int. J. Biol. Macromol.*, 2020, **160**, 340–351.
  - 56 A. Khazaei, L. Nateghi, N. Zand, A. Oromiehie and F. Garavand, *J. Polym.*, 2021, **13**(16), 2778.
  - 57 P. Singh, G. Kaur, A. Singh and P. Kaur, *J. Food Meas. Charact.*, 2023, **17**(1), 527–545.
  - 58 Q. Liu, R. Han, D. Yu, Z. Wang, X. Zhuansun and Y. Li, *LWT–Food Sci. Technol.*, 2024, **191**, 115686.
  - 59 S. M. Amaraweera, C. Gunathilake, O. H. Gunawardene, N. M. Fernando, D. B. Wanninayaka, A. Manamperi, R. S. Dassanayake, S. M. Rajapaksha, M. Gangoda, C. Fernando, A. K. Kulatunga and A. Manipura, *Cellulose*, 2021, **28**, 10531–10548.
  - 60 N. Karimi-Khorrami, M. Radi, S. Amiri, E. Abedi and D. J. McClements, *Int. J. Biol. Macromol.*, 2022, **207**, 801–812.
  - 61 Y. Zhou, X. Wu, J. Chen and J. He, *Int. J. Biol. Macromol.*, 2021, **184**, 574–583.
  - 62 M. Zhang and H. Chen, *Int. J. Biol. Macromol.*, 2023, **233**, 123462.
  - 63 E. P. da Cruz, J. B. Pires, F. N. dos Santos, L. M. Fonseca, M. Radünz, J. Dal Magro, E. A. Gandra, E. Zavareze and A. R. G. Dias, *Food Hydrocolloids*, 2023, **145**, 109105.
  - 64 T. J. Gutiérrez, *J. Polym. Environ.*, 2018, **26**(9), 3902–3912.
  - 65 Y. Zhang, Y. Pu, H. Jiang, L. Chen, C. Shen, W. Zhang, J. Cao and W. Jiang, *Food Chem.*, 2024, **435**, 137534.
  - 66 J. Xiao, C. Gu, D. Zhu, Y. Huang, Y. Luo and Q. Zhou, *LWT–Food Sci. Technol.*, 2021, **140**, 110809.
  - 67 A. Hejna, J. Lenža, K. Formela and J. Korol, *J. Polym. Environ.*, 2019, **27**, 1112–1126.
  - 68 H. Haghighi, S. Biard, F. Bigi, R. De Leo, E. Bedin, F. Pfeifer, H. W. Siesler, F. Licciardello and A. Pulvirenti, *Food Hydrocolloids*, 2019, **95**, 33–42.
  - 69 X. He, M. Li, X. Gong, B. Niu and W. Li, *Food Packag. Shelf Life*, 2021, **29**, 100697.
  - 70 H. Bansal, H. P. Singh, S. Singh, A. Sharma, J. Singh, K. Kaur and S. K. Mehta, *Int. J. Biol. Macromol.*, 2024, 133239.
  - 71 A. Amalraj, J. T. Haponiuk, S. Thomas and S. Gopi, *Int. J. Biol. Macromol.*, 2020, **151**, 366–375.
  - 72 P. B. Kavur and A. Yemenicioğlu, *Food Hydrocolloids*, 2024, **151**, 109790.
  - 73 J. Y. Zhu, C. H. Tang, S. W. Yin and X. Q. Yang, *Carbohydr. Polym.*, 2018, **181**, 727–735.
  - 74 J. Andrade, C. González-Martínez and A. Chiralt, *Food Packag. Shelf Life*, 2022, **33**, 100855.
  - 75 S. Li, Y. Jiang, Y. Zhou, R. Li, Y. Jiang, M. A. Hossen, J. Dai, W. Qin and Y. Liu, *Food Chem.*, 2022, **370**, 131082.
  - 76 B. Ashaq, K. Rasool, S. Habib, I. Bashir, N. Nisar, S. Mustafa, Q. Ayas, G. A. Nayik, J. Uddin, S. Ramniwas, R. Mugabi and S. M. Wani, *Food Chem. X*, 2024, 101521.
  - 77 R. K. Basha, N. F. Abuhan, S. H. Othman, N. Z. N. Hasnan, R. Sukor, N. S. Azmi, N. A. M. Amin and Z. M. Dom, *Adv. Agric. Food Res. J.*, 2020, **1**, 2.
  - 78 M. A. Abou-Raya, M. M. Khalil, A. H. S. Soliman and R. AbdElmoula, *J. Food Dairy Sci.*, 2023, **14**(11), 251–260.
  - 79 S. Sharma, S. Habib, D. Sahu and J. Gupta, *Med. Chem.*, 2021, **17**(1), 2–12.
  - 80 M. Alagawany, M. T. El-Saadony, S. S. Elnesr, M. Farahat, G. Attia, M. Madkour and F. M. Reda, *Poult. Sci.*, 2021, **100**(6), 101172.
  - 81 I. K. Sani, S. P. Geshlaghi, S. Pirs and A. Asdaghi, *Food Hydrocolloids*, 2021, **117**, 106719.
  - 82 M. I. Socaciu, M. Fogarasi, C. A. Semeniuc, S. A. Socaci, M. A. Rotar, V. Mureşan, O. L. Pop and D. C. Vodnar, *Polymers*, 2020, **12**(8), 1748.

